Processing and Application of Ceramics 13 [3] (2019) 244–249
https://doi.org/10.2298/PAC1903244Z

Electrical properties of Cu-Mn-Zr co-doped ceria electrolytes for intermediate temperature solid oxide fuel cell application

Igor V. Zagaynov*, Sergey V. Fedorov, Margarita A. Goldberg

Baikov Institute of Metallurgy and Materials Science, Leninskii Pr. 49, Moscow, Russia

Received 10 January 2019; Received in revised form 24 April 2019; Accepted 18 July 2019

Abstract

Nanocrystalline triple-doped ceria based solid electrolyte materials ($Cu_xMn_{0.1-x}Zr_{0.1}Ce_{0.8}O_2$, where x = 0, 0.02, 0.04, 0.06, 0.08 and 0.1, as well as $Cu_{0.08}Mn_{0.02}Zr_yCe_{0.9-y}O_2$, where y = 0 and 0.1) for intermediate temperature solid oxide fuel cells were successfully synthesized by co-precipitation method with sonication and sintered at 1150 °C for 4 h in air. Relative densities of all the samples were above 90–96%. All systems were characterized by XRD, SEM-EDS and TG-DSC-MS for the investigation of structure and microstructure with elemental composition. The electrical conductivity of these materials was measured by AC impedance spectroscopy in the temperature range of 500–750 °C in air. It was shown that $Cu_{0.08}Mn_{0.02}Zr_{0.1}Ce_{0.8}O_2$ ceramics possessed the maximum conductivity of $8 \cdot 10^{-3}$ S/cm at 600 °C in air.

Keywords: *CeO_2, ionic conductivity, impedance spectroscopy, IT-SOFC*

I. Introduction

Fuel cells are electrochemical energy conversion devices that convert chemical energy from the fuel directly into electricity (and heat) without involving the process of combustion. Among many types of sustainable energy sources, SOFC (solid oxide fuel cell) devices have shown the highest performance, the most efficient and the cleanest power-generation in the applied technology. There is no optimal operating temperature for fuel cells. The appropriate fuel cell technology to choose for a given application is a function of the required performance, lifetime, cost, fuel, size, weight, efficiency, start-up time, waste heat quality, etc. However, it is clear that lowering the operating temperature of SOFC can unlock a wider range of potential applications, including some that have previously been the domain of low temperature fuel cells [1,2]. There is a trend to move to lower temperatures of operation, into the so-called intermediate temperature (IT-SOFC) range of 500–750 °C [3,4].

Most attention is paid to the development of electrolytes for IT-SOFC. The properties of the electrolyte have a major impact on fuel cell performance and this electrolyte should have the following characteristics: high oxide ion conductivity (> 10^{-3} S/cm) and low electronic conductivity; excellent thermal and chemical stability in relation to the reactant environment and the contacting electrode materials; low cost and environmentally benign [5].

Doped ceria is considered to be a promising electrolyte. It was demonstrated that the maximum ionic conductivity occurred at 10–20 mol% doped systems. A range of dopant cations, especially cations of rare-earth elements (REE), has been investigated and it was found that samarium (SDC) and gadolinium doped ceria (GDC) are the most promising, but the cost of rare-earth oxides is very high [6–8]. Co-doping enhances the ionic conductivity of ceria-based electrolytes. A decrease in the total conductivity and an increase in the activation energy of Sm^{3+} and Gd^{3+} co-doped ceria electrolyte were demonstrated because of the decreased mobility of oxygen vacancies [9,10].

The potential of co-doping for the enhancement of the ionic conductivity of doped ceria based electrolytes should be further explored by selecting suitable co-dopants. Thus, it is necessary to investigate ceramics based on ceria solid solutions (using low-cost dopants) as a promising electrolyte for IT-SOFC. A more affordable approach is to introduce sintering additives into the starting material. The results of studies of the influence on the sintering and the conductivity of GDC of

* Corresponding authors: tel: +7 499 1352060,
e-mail: *igorscience@gmail.com*

cobalt, copper, manganese, iron and nickel oxides were obtained. It is shown that the introduction of these additives in the amount of 1–5 mol% significantly increases the rate of shrinkage, reduces the sintering temperature and increases the total conductivity. In this case, the greatest effect is achieved when Cu and Mn are introduced [11–17]. In general, the addition of transition metal oxides enhances the densification rate of ceria. However, almost all of these activators exert an undesirable effect in the electrical property by increasing the electronic component of the conductivity. To solve this problem, it is proposed to use solid solutions (in this work containing Mn, Cu and Zr), which will provide high density and ionic conductivity.

II. Materials and methods

Cu-Mn-Zr co-doped ceria ceramic powders with different compositions ($Cu_xMn_{0.1-x}Zr_{0.1}Ce_{0.8}O_2$, where x = 0, 0.02, 0.04, 0.06, 0.08 and 0.1, as well as $Cu_{0.08}Mn_{0.02}Zr_yCe_{0.9-y}O_2$, where y = 0 and 0.1) were synthesized by co-precipitation method. Stoichiometric amounts of precursor salts ($Ce(NO_3)_3 \cdot 6\,H_2O$, $ZrO(NO_3)_2 \cdot 7\,H_2O$, $Cu(NO_3)_2 \cdot 3\,H_2O$, $Mn(NO_3)_2 \cdot 4\,H_2O$ purchased from Acros Organics, 99.9%) were dissolved in concentrated nitric acid (68%) with the salt concentration of 0.667 M. After dissolution of salts, this mixture was added to distilled water, giving concentration of 0.1 M. Then, the co-precipitation was carried out by the addition of 2.5 M KOH solution up to pH = 11. Ultrasonic processing (35 kHz, 150 W) was used during the entire process at 30 °C under stirring. The resulting precipitates were filtered, washed with distilled water-ethanol solution (volume ratio of H_2O/C_2H_5OH = 9), dried at 150 °C for 12 h and calcined in static air by heating at a rate of 4 °C/min from room temperature to 500 °C and kept at 500 °C for 1 h in the muffle furnace [18].

The as-obtained powders were pressed into pellets (with 10 wt.% binder made of 5 wt.% aqueous solution of polyvinyl alcohol) with 5 mm in diameter and 2 mm in thickness at 71 MPa. The pressed pellets were sintered at 1150 °C for 4 h in air with heating rate of 4 °C/min.

All powders and ceramics were characterized by XRD (Rigaku MiniFlex 600, CuKα radiation). Crystallite sizes (d_{XRD}) were determined by the Scherrer equation using the full-width at half maximum after accounting for instrumental broadening with germanium as reference. The average crystallite sizes were calculated not on a separate peak, but with all planes during the fitting of the spectrum. Thermal analyses were performed by TG-DSC-MS (Netzsch STA449F3) and the samples were heated to 1350 °C at the rate of 10 /min in air. Microstructure of the sintered samples was investigated by SEM-EDS (TESCAN VEGA II SBU with INCA Energy 300 energy dispersive spectrometers).

Symmetric cells for the impedance studies (Elins Z-350M impedance meter, the frequency range from 0.1 Hz to 4 MHz at the amplitude of AC signal of 30 mV) were prepared by deposition (brushing) of platinum paste onto both sides of the electrolyte pellets, drying at 150 °C for 1 h and annealing at 900 °C for 4 h in air. A platinum wire was used as current collector. To separate the ionic contribution from total conductivity, Wagner's polarization technique with an electrical loader (Solartron 1285A Potentiostat) was used to calculate the ionic transport number by imposing an external fixed DC voltage (1.5 V) across the electrolyte (DC current was monitored as a function of time on application of a fixed DC voltage across the symmetric C|electrolyte|C cell) [19,20].

III. Results and discussion

3.1. Microstructure

It is observed that the pellets could be sintered almost to its theoretical density value at low temperatures (i.e. at 1150 °C). According to TG-DSC (Fig. 1), this temperature is sufficient to remove surface residual components (H_2O and CO_2 formation) and form dense ceramics.

The XRD patterns of the sintered electrolytes are shown in Fig. 2. All peaks reflect the typical fluorite structure of ceria. The average crystallite size calculated using Scherrer formula was about 7–9 nm for the synthesized powders (Table 1). This also affected the formation of a small amount of the individual copper oxide phase (~3 wt.%) in the samples with higher Cu-doping (x = 0.1). The elemental compositions of the sintered pellets were determined through EDS analysis. The mole fractions in all the compositions were either equal or nearly equal to nominal with a small excess of copper, since it is known that copper is located mainly

Table 1. Some samples' characteristics

Sample	d_{XRD} [nm] (powder)	a [nm] (powder)	a [nm] (ceramics)	Relative density [%TD]	E_a [eV]
$Mn_{0.1}Zr_{0.1}Ce_{0.8}O_2$	7	5.3816	5.3777	96	1.66
$Cu_{0.02}Mn_{0.08}Zr_{0.1}Ce_{0.8}O_2$	6	5.3781	5.3703	92	1.50
$Cu_{0.04}Mn_{0.06}Zr_{0.1}Ce_{0.8}O_2$	7	5.3788	5.3739	92	1.46
$Cu_{0.06}Mn_{0.04}Zr_{0.1}Ce_{0.8}O_2$	7	5.3832	5.3766	93	0.87
$Cu_{0.08}Mn_{0.02}Zr_{0.1}Ce_{0.8}O_2$	8	5.3845	5.3792	96	0.37
$Cu_{0.08}Mn_{0.02}Ce_{0.9}O_2$	9	5.4064	5.4092	90	0.63
$Cu_{0.1}Zr_{0.1}Ce_{0.8}O_2$	8	5.3886	5.3730	91	1.16

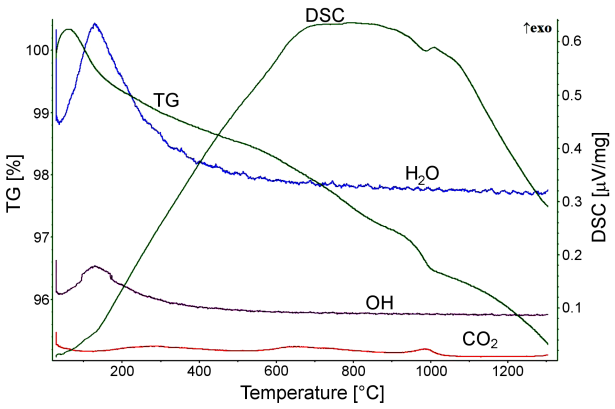

Figure 1. TG-DSC-MS data of sample $Cu_{0.08}Mn_{0.02}Zr_{0.1}Ce_{0.8}O_2$

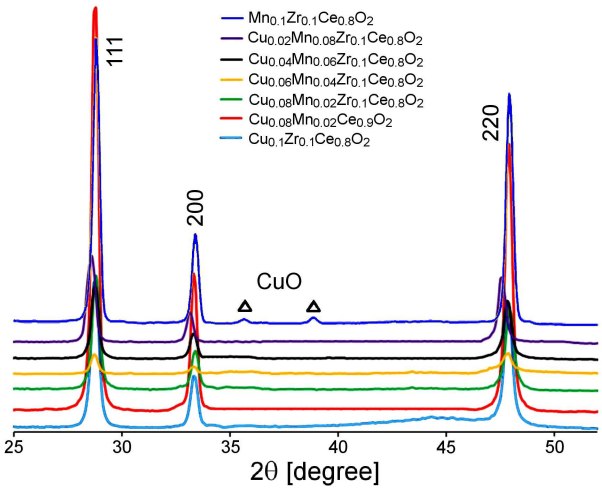

Figure 2. XRD patterns of sintered ceramics

on the ceria surfaces of the lattice, which was previously confirmed by XPS method [21]. The change in the lattice parameter of the sintered samples in comparison to those for the synthesized powder was observed (Table 1). Thus, the decrease in the crystal lattice parameter *a* was observed, which could be associated with an increase in the degree of incorporation of dopants into the crystal lattice (Table 1). The incorporation of dopants in the ceria crystalline lattice is also confirmed with the shift of XRD peaks, which is the most obvious when smaller Zr replace Ce cations (i.e. the samples $Cu_{0.08}Mn_{0.02}Ce_{0.9}O_2$ and $Cu_{0.08}Mn_{0.02}Ce_{0.8}Zr_{0.1}O_2$).

The samples heated at 1150 °C have the relative density of 90–96 %TD, calculated as the ratio of densities determined by hydrostatic weighing and XRD based cell parameter. Microstructural analysis of the samples by SEM (Fig. 3) demonstrated that the average grain size was less than 2 μm. The absence of pores in the images of the microstructure also confirms the high density of the obtained materials.

3.2. Impedance analyses

The results of the total ionic conductivity measurements performed in air at different temperatures (from 500 to 750 °C) are presented in Fig. 4. The sample with the lowest conductivity value is the copper-free system ($Mn_{0.1}Zr_{0.1}Ce_{0.8}O_2$). Improved conductivity was observed after the addition of copper. The maximum conductivity was found for the sample $Cu_{0.08}Mn_{0.02}Zr_{0.1}Ce_{0.8}O_2$ and at 600 °C it was $\sigma_{600\,°C} = 8 \cdot 10^{-3}$ S/cm. A sharp decrease in the electrical conductivity was observed in the sample with higher Cu-doping (i.e. $Cu_{0.1}Zr_{0.1}Ce_{0.8}O_2$) and this is due to the formation of CuO phase. The addition of zirconium is known to be beneficial as a high-temperature stabilizer of ceria lattice ($T > 700$ °C), which is also observed. Thus, the sample without Zr ($Cu_{0.08}Mn_{0.02}Ce_{0.9}O_2$) showed a lower electrical conductivity (less than 5 times). These results demonstrate that co-doping with the optimal ratio can improve the conductivity of ceria based electrolytes. When compared with other electrolytes, sintered even at a higher temperature, the electrical conductivity of the developed systems is comparable or higher than samples doped with REE at 600 °C [22–30].

Activation energies (E_a) of samples were calculated from the graphs using the following Arrhenius-Frenkel relation:

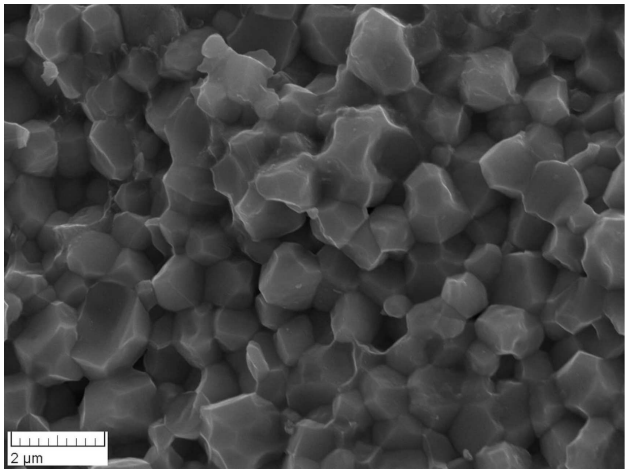

Figure 3. SEM micrograph of $Cu_{0.08}Mn_{0.02}Zr_{0.1}Ce_{0.8}O_2$ ceramics

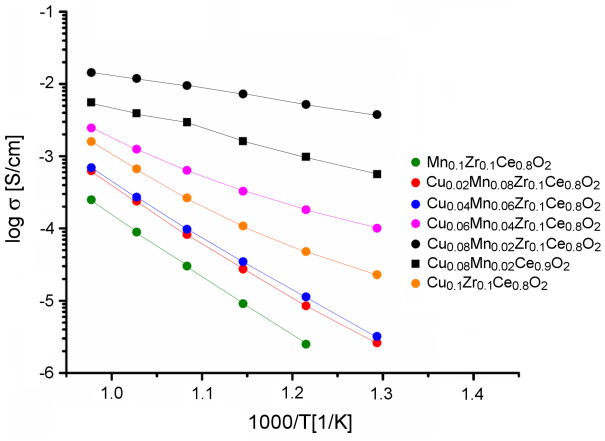

Figure 4. The total electrical conductivity of ceramics as a function of temperature

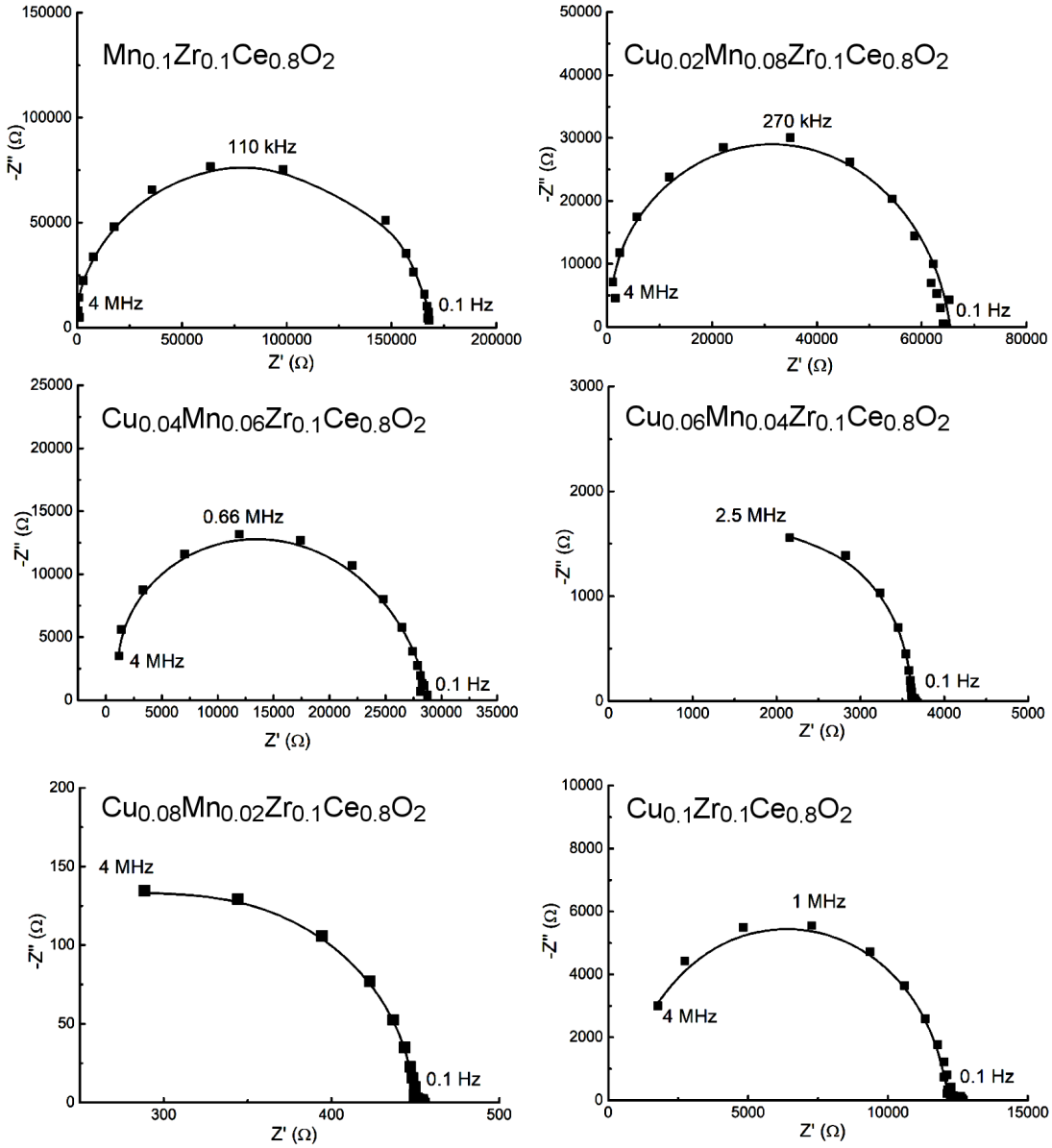

Figure 5. Complex impedance spectra measured at 600 °C in air of the sintered samples

$$\sigma \cdot T = \sigma_0 \cdot \exp\left(-\frac{E_a}{k \cdot T}\right) \quad (1)$$

The calculated activation energies (E_a) for all samples are represented in Table 1. The minimum value of activation energy for the sample $Cu_{0.08}Mn_{0.02}Zr_{0.1}Ce_{0.8}O_2$ may be due to the interaction between concentrated oxygen vacancies and dopant cations in the lattice [31].

The increase in the concentration of mobile ions (oxygen vacancies) leads to the enhanced ionic conductivity of doped ceria. The decreased mobile oxygen vacancies lead to decrease in the total ionic conductivity due to the formation of local defects in the ceria structure, i.e. at higher dopant concentrations, the increased probability of dopant clusters lead to formation of deep traps that accommodate the oxygen vacancies and restrict the diffusion of oxygen vacancies [22]. The highest ionic conductivity is achieved when the sample possesses both the lowest activation energy of conduction and the highest pre-exponential term. It is well known that the ionic conduction in doped ceria occurs by oxygen ion migration via a vacancy mechanism, and it is mainly determined by the Coulombic interactions between defects having opposite charges: positively charged oxygen vacancies and negatively charged dopant. These associations of defects dissociate with the increase in temperature, releasing mobile charge carriers. In the sample $Cu_{0.08}Mn_{0.02}Zr_{0.1}Ce_{0.8}O_2$, the activation energy of conduction has the dominating effect on the conductivity, which is associated with the binding energy of defect clusters (dopants and associated oxygen vacancies). A study has shown that doped ceria-based electrolytes exhibit electronic conductivity mainly at high temperatures (>1000 °C) [3]. Moreover, the oxide ion transference number of co-doped ceria electrolytes was 0.86–0.94 at 600 °C, and slightly in-

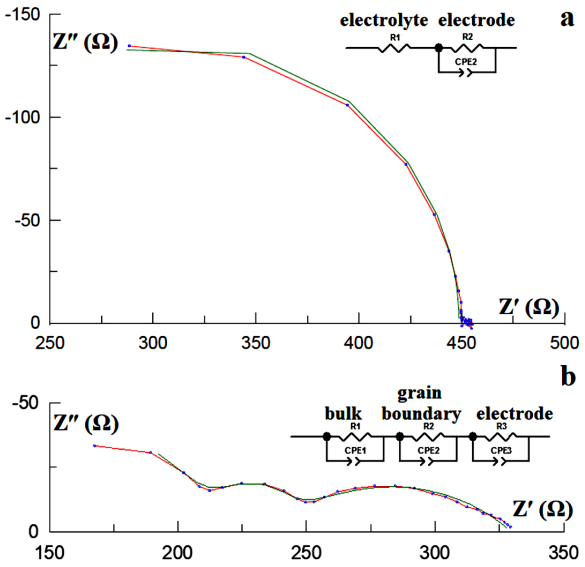

Figure 6. Complex impedance spectra at 600 °C in air of sample: a) $Cu_{0.08}Mn_{0.02}Zr_{0.1}Ce_{0.8}O_2$ and b) $Cu_{0.08}Mn_{0.02}Ce_{0.9}O_2$

creased as the temperature increased.

Impedance graphs of the sintered samples at temperature 600 °C are shown in Figs. 5 and 6. Generally, impedance spectra consist of graphs with real part Z' on x-axis and negative imaginary part Z'' on y-axis known as complex impedance spectra and they are materials characteristics giving the conducting nature. The complex impedance plot (the Nyquist plot) of an electrolyte material is generally characterized by three successive semicircles: grain (bulk; higher frequency), grain boundary (moderate frequency), and electrode (lower frequency) contributions. In the frequency range from 0.1 Hz to 4 MHz, one impedance semicircle is observed (Fig. 5), where semicircle is attributed to the electrode polarization resistivity, associated with the chemical reaction between adsorbed O_2 molecules and electrons to form oxide ions at the interface ($O_2 + 4\,e^- \longrightarrow 2\,O^{2-}$). The total impedances decreased with increasing temperature and shifted to a higher frequency (at temperatures 500–750 °C, not shown). The bulk resistance (R_g) and grain boundary resistance (R_{gb}) contributions were not well resolved due to their similar relaxation times of charge carriers in both bulk and grain boundaries [32]. Nevertheless, for the sample $Cu_{0.08}Mn_{0.02}Ce_{0.9}O_2$ (Fig. 6b) there are three semicircles, which consists of three parallel resistances (R) and constant phase elements (CPE) connected in series. In the temperature range of measurements the impedance diagrams show similar features and the electrode resistance decreases with the temperature increase.

IV. Conclusions

The Mn-Cu-Zr co-doped ceria electrolytes were successfully prepared by the simple co-precipitation method and sintered at a low temperature of 1150 °C for 4 h in air. All samples were characterized by powder X-ray diffraction, scanning electron microscope and energy dispersive spectroscopy. The sintered samples are fluorite-type ceria-based solid solutions and they have single phase cubic structure with dense microstructure. The results showed that the system $Cu_{0.08}Mn_{0.02}Zr_{0.1}Ce_{0.8}O_2$ possessed the maximum conductivity of $8 \cdot 10^{-3}$ S/cm at 600 °C in air. The prospect of using transition metals as dopants was demonstrated. For the material's cost, these elements are more economically viable than rare earth elements.

Acknowledgement: This research was supported by Russian Science Foundation (No. 17-73-10331).

References

1. D.J.L. Brett, A. Atkinson, N.P. Brandon, S.J. Skinnerd, "Intermediate temperature solid oxide fuel cells", *Chem. Soc. Rev.*, **37** (2008) 1568–1578.
2. A.M. Abdalla, S. Hossain, A.T. Azad, P.M.I. Petra, F. Begum, S.G. Eriksson, A.K. Azad, "Nanomaterials for solid oxide fuel cells: A review", *Renew. Sustain. Energy Rev.*, **82** (2018) 353–368.
3. B.C.H. Steele, "Material science and engineering: The enabling technology for the commercialisation of fuel cell systems", *J. Mater. Sci.*, **36** (2001) 1053–1068.
4. L. Fan, B. Zhu, P.-C. Su, C. He, "Nanomaterials and technologies for low temperature solid oxide fuel cells: Recent advances, challenges and opportunities", *Nano Energy*, **45** (2018) 148–176.
5. J.B. Goodenough, "Oxide-ion electrolytes", *Annu. Rev. Mater. Res.*, **33** (2003) 91–128.
6. S. Dikmen, H. Aslanbay, E. Dikmen, O. Şahin, "Hydrothermal preparation and electrochemical properties of Gd^{3+} and Bi^{3+}, Sm^{3+}, La^{3+}, and Nd^{3+} codoped ceria-based electrolytes for intermediate temperature-solid oxide fuel cell", *J. Power Sources*, **195** (2010) 2488–2495.
7. W. Zhao, S. An, L. Ma, "Processing and characterization of Bi_2O_3 and Sm_2O_3 codoped CeO_2 electrolyte for intermediate-temperature solid oxide fuel cell", *J. Am. Ceram. Soc.*, **94** (2011) 1496–1502.
8. Sk. Anirban, A. Dutta, "Structural and ionic transport mechanism of rare earth doped cerium oxide nanomaterials: Effect of ionic radius of dopant cations", *Solid State Ionics*, **309** (2017) 137–145.
9. M. Anwara, M. S.A. Ali, N.A. Baharuddin, N.F. Raduwan, A. Muchtar, M.R. Somalu, "Structural, optical and electrical properties of $Ce_{0.8}Sm_{0.2-x}Er_xO_{2-\delta}$ (x = 0–0.2) co-doped ceria electrolytes", *Ceram. Int.*, **44** (2018) 13639–13648.
10. L.B. Winck, J.L. de A. Ferreira, J.M.G. Martinez, J.A. Araujo, A.C.M. Rodrigues, C.R.M. da Silva, "Synthesis, sintering and characterization of ceria-based solid electrolytes codoped with samaria and gadolinium using the Pechini method", *Ceram. Int.*, **43** (2017) 16408–16415.
11. C. Kleinlogel, L.J. Gauckler, "Mixed electronic-ionic conductivity of cobalt doped cerium gadolinium oxide", *J. Electroceram.*, **5** (2000) 231–243.
12. C. Kleinlogel, L.J. Gauckler, "Sintering of nanocrystalline CeO_2 ceramics", *Adv. Mater.*, **13** (2001) 1081–1085.
13. D.P. Fagg, V.V. Kharton, J.R. Frade, "P-type electronic transport in $Ce_{0.8}Gd_{0.2}O_{2-\delta}$: The effect of transition metal

oxide sintering aids", *J. Electroceram.*, **9** (2002) 199–207.
14. E.Yu. Pikalova, A.N. Demina, A.K. Demin, A.A. Murashkina, V.E. Sopernikov, N.O. Esina, "Effect of doping with Co_2O_3, TiO_2, Fe_2O_3, and Mn_2O_3 on the properties of $Ce_{0.8}Gd_{0.2}O_{2-\delta}$", *Inorg. Mater.*, **43** (2007) 735–742.
15. A.V. Nikonov, A.V. Spirin, V.R. Khrustov, S.N. Paranin, N.B. Pavzderin, K.A. Kuterbekov, T.N. Nurakhmetov, Y.K. Atazhan, "Synthesis and properties of solid electrolyte $Ce_{0.9}Gd_{0.1}O_{2-\delta}$ with Co, Cu, Mn, Zn doping", *Inorg. Mater.*, **52** (2016) 708–715.
16. E.L. Santos, R. Muccillo, E.N.S. Muccillo, "Densification and electrical conductivity of Mn-doped CeO_2", *Mater. Sci. Forum*, **591-593** (2008) 639–643.
17. B. Ji, C. Tian, C. Wang, T. Wu, J. Xie, M. Li, "Preparation and characterization of $Ce_{0.8}Y_{0.2-x}Cu_xO_{2-\delta}$ as electrolyte for intermediate temperature solid oxide fuel cells", *J. Power Sources*, **278** (2015) 420–429.
18. I.V. Zagaynov, A.A. Konovalov, E.A. Koneva, "Investigation of structure and morphology of Cu-Mn-Zr-Ce-O solid solutions", *Lett. Mater.*, **8** (2018) 135–139.
19. S. Ramesh, K.C.J. Raju, "Preparation and characterization of $Ce_{1-x}(Gd_{0.5}Pr_{0.5})_xO_2$ electrolyte for IT-SOFCs", *Int. J. Hydrogen Energy*, **37** (2012) 10311-10317.
20. L. Spiridigliozzi, G. Dell'Agli, G. Accardo, S.P. Yoon, D. Frattini, "Electro-morphological, structural, thermal and ionic conduction properties of Gd/Pr co-doped ceria electrolytes exhibiting mixed Pr^{3+}/Pr^{4+} cations", *Ceram. Int.*, **45** (2019) 4570–4580.
21. I.V. Zagaynov, A.V. Naumkin, Yu.V. Grigoriev, "Perspective intermediate temperature ceria based catalysts for CO oxidation", *Appl. Cat. B*, **236** (2018) 171–175.
22. K. Venkataramana, C. Madhuri, Y.S. Reddy, G. Bhikshamaiah, C.V. Reddy, "Structural, electrical and thermal expansion studies of tri-doped ceria electrolyte materials for IT-SOFCs", *J. Alloy. Compd.*, **719** (2017) 97–107.
23. A. Arabaci, "Effect of Er, Gd, and Nd co-dopants on the properties of Sm-doped ceria electrolyte for IT-SOFC", *Metall. Mater. Trans. A*, **48** (2017) 2282–2288.
24. T.H. Santos, J.P.F. Grilo, F.J.A. Loureiro, D.P. Fagg, F.C. Fonseca, D.A. Macedo, "Structure, densification and electrical properties of Gd^{3+} and Cu^{2+} co-doped ceria solid electrolytes for SOFC applications: Effects of Gd_2O_3 content", *Ceram. Int.*, **44** (2018) 2745–2751.
25. Y. Gan, J. Cheng, M. Li, H. Zhan, W. Sun, "Enhanced ceria based electrolytes by codoping samaria and scandia for intermediate temperature solid oxide fuel cells", *Mater. Chem. Phys.*, **163** (2015) 279–285.
26. M. Stojmenović, M. Žunić, J. Gulicovski, D. Bajuk-Bogdanović, I. Holclajtner-Antunović, V. Dodevski, S. Mentus, "Structural, morphological, and electrical properties of doped ceria as a solid electrolyte for intermediate-temperature solid oxide fuel cells", *J. Mater. Sci.*, **50** (2015) 3781–3794.
27. L. Xiaomin, L. Qiuyue, Z. Lili, L. Xiaomei, "Synthesis and characterization of $Ce_{0.8}Sm_{0.2-x}Pr_xO_{2-\delta}$ (x = 0.02–0.08) solid electrolyte materials", *J. Rare Earths*, **33** (2015) 411–416.
28. Z. Tao, H. Ding, X. Chen, G. Hou, Q. Zhang, M. Tang, W. Gu, "The co-doping effect of Sm and In on ceria for electrolyte application in IT-SOFC", *J. Alloy. Compd.*, **663** (2016) 750–754.
29. I.V. Zagaynov, S.V. Fedorov, A.A. Konovalov, O.S. Antonova, "Perspective ceria-based solid solutions $Gd_xBi_{0.2-x}Ce_{0.8}O_2$", *Mater. Lett.*, **203** (2017) 9–12.
30. K.C. Anjaneya, M.P. Singh, "Synthesis and properties of gadolinium doped ceria electrolyte for IT-SOFCs by EDTA-citrate complexing method", *J. Alloy. Compd.*, **695** (2017) 871–876.
31. S. Ramesh, V.P. Kumar, P. Kistaiah, C.V. Reddy, "Preparation, characterization and thermos electrical properties of co-doped $Ce_{0.8-x}Sm_{0.2}Ca_xO_{2-\delta}$ materials", *Solid State Ionics*, **181** (2010) 86–91.
32. Y.-C. Wu, C.-C. Lin, "The microstructures and property analysis of aliovalent cations (Sm^{3+}, Mg^{2+}, Ca^{2+}, Sr^{2+}, Ba^{2+}) co-doped ceria-base electrolytes after an aging treatment", *Int. J. Hydrogen Energy*, **39** (2014) 7988–8001.